REALISTIC ADVANCEMENT FOR NICKEL-BASED SINGLE CRYSTAL SUPERALLOYS BY THE d-ELECTRONS CONCEPT

K. Matsugi, Y. Murata*, M. Morinaga* and N. Yukawa*

Graduate school, Toyohashi University of Technology
*Department of Production Systems Engineering,
Toyohashi University of Technology,
Toyohashi, Aichi 441, Japan

Abstract

We have proposed the d-electrons concept for the design and development of nickel-based single crystal superalloys. In this concept, two alloying parameters has been determined by the molecular orbital calculation (DV-Xα cluster calculation). The one is the d-orbital energy level (Md) of alloying transition element, and the other is the bond order (Bo) between atoms. The compositional average of Md and Bo parameters are denoted as $\overline{Md}$ and $\overline{Bo}$, respectively.

In this study, several alloying effects on the high temperature properties were investigated with the aid of these d-electrons parameters, $\overline{Md}$ and $\overline{Bo}$. For example, it was found that the γ' solvus temperature was predictable by using these parameters. An idea about alloying vectors was introduced newly to the d-electrons concept. Using this idea, the trend for the partitioning of the alloying elements between the γ and the γ' phases could be understood consistently. Also, the alloying effects of Cr, Co, Re, Ti and Hf were shown on the creep-rupture property and the hot-corrosion resistance of superalloys. In addition, it was found that the realistic advancement for nickel-based superalloys was well recognized using the $\overline{Bo}$-$\overline{Md}$ diagram. All the single crystal superalloys so far developed and the high strength conventional cast alloys were localized in a very small region in the $\overline{Bo}$-$\overline{Md}$ diagram. On the basis of these results, a proposal was discussed for the development and the modification of single crystal superalloys, in particular, of the Re-containing single crystal superalloys.

Superalloys 1992
Edited by S.D. Antolovich, R.W. Stusrud, R.A. MacKay,
D.L. Anton, T. Khan, R.D. Kissinger, D.L. Klarstrom
The Minerals, Metals & Materials Society, 1992

Introduction

The d-electrons concept has been devised on the basis of the molecular orbital calculations of electronic structures (1-4). Employing this concept, we have developed several nickel-based single crystal superalloys (TUT alloys) (5,6). Some of them are shown in Table 1 together with other single crystal superalloys, PWA alloys and CMSX alloys. Our designed alloys, TUT 92, TUT 31D and TUT 95, have an excellent combination of creep-rupture properties, hot-corrosion resistance, low density and low materials cost. In this regard, these alloys are much superior to PWA 1480, PWA 1484, CMSX-2 and CMSX-4. Thus, the d-electrons concept is very useful in designing superalloys. The purposes of this study are two-fold. The one purpose is to understand respective alloying effects on high temperature properties using this concept. The another purpose is to look over the realistic advancement in single crystal superalloys from a view of this concept in order to find an alternative way for new alloy development of superalloys.

Table 1 Compositions of the typical single crystal superalloys.

alloy	composition , mol%									
	Ni	Cr	Al	Ti	Ta	W	Mo	Re	Co	other
TUT 92	bal.	10	12	1.5	2.1	2.3	0.8	0.25	—	
TUT 31D	bal.	10	12	1.5	2.3	2.5	0.8	0.25	—	
TUT 95	bal.	10	12	1.5	2.7	2.3	0.8	0.25	—	
PWA 1480	bal.	12	11	1.9	4.0	1.3	—	—	5.2	
PWA 1484	bal.	6	13	—	3.0	2.0	1.3	1.0	11	0.04Hf
CMSX-2	bal.	7	12	1.3	2.0	2.6	0.4	—	4.7	
CMSX-4	bal.	8	13	1.3	2.2	2.1	0.4	1.0	10	

The d-electrons Concept

The main alloying elements of superalloys are transition elements with unpaired d-electrons. High cohesive energy of transition metals and alloys can be attributed to the covalent bond strength between the d-electrons. Therefore, it is important to understand the bond nature of the d-electrons between the atoms in superalloys.

We have simulated the d-electrons state by using a molecular orbital method (the DV-Xα cluster method) (7), and determined two new alloying parameters. The one is the d-orbital energy level (Md) of alloying transition element. This Md is known to correlate with the electronegativity and the atomic radius of elements (1). The other is the bond order (Bo) that is a measure of the covalent bond strength between the Ni atom and the alloying element in superalloys. The values of the parameters for each element are listed in Table 2.

Table 2 List of Md and Bo values.

Element		Md / Bo	Element		Md / Bo
3d	Ti	2.271/1.098	4d	Zr	2.944/1.479
	V	1.543/1.141		Nb	2.117/1.594
	Cr	1.142/1.278		Mo	1.550/1.611
	Mn	0.957/1.001	5d	Hf	3.020/1.518
	Fe	0.858/0.857		Ta	2.224/1.670
	Co	0.777/0.697		W	1.655/1.730
	Ni	0.717/0.514		Re	1.267/1.692
	Cu	0.615/0.272	others	Al	1.900/0.533
				Si	1.900/0.589

For alloy, the average values of Md and Bo are defined by taking the compositional average, and $\overline{Md}$ and $\overline{Bo}$ are denoted as follows:

$$\overline{Md} = \Sigma Xi(Md)i, \quad (1)$$

$$\overline{Bo} = \Sigma Xi(Bo)i. \quad (2)$$

Here, Xi is the atomic fraction of component i in the alloy, (Md)i and (Bo)i are the Md and Bo values for component i, respectively. Once the alloy composition is given, the $\overline{Md}$ and $\overline{Bo}$ values are simply calculated by using these equations.

The new PHACOMP has been proposed using the $\overline{Md}$ parameter (2). Compared to the current Nv-PHACOMP, it provides a more accurate prediction method for the occurrence of topologically close packed (TCP) phases in superalloys. The another parameter, $\overline{Bo}$, is considered to be related in some way to the strength of alloys. It is generally known that the elements of high Bo values are the principal alloying elements in any structual alloys (2). As shown in Table 2, the high Bo elements in superalloys are Cr (3d elements), Mo (4d elements) and Ta, W, Re (5d elements).

$\overline{Bo}$-$\overline{Md}$ Diagram and Alloying Vectors

First, the validity of the d-electrons concept will be shown using one example. In Fig.1 nineteen conventional cast superalloys are plotted in the $\overline{Bo}$-$\overline{Md}$ diagram. The contour lines with respect to 0.2% yield stress at 1255K (8) are also shown by the broken lines. The 0.2% yield stress shows the maximum at the $\overline{Md}$ value of about 0.98 [eV] and the $\overline{Bo}$ value of about 0.67. Furthermore, twenty-one single crystal superalloys, which have been developed so far in the world, are located near the maximum position as is represented by the shadow area in Fig.1. Thus, a target region for alloy design can be specified on the $\overline{Bo}$-$\overline{Md}$ diagram.

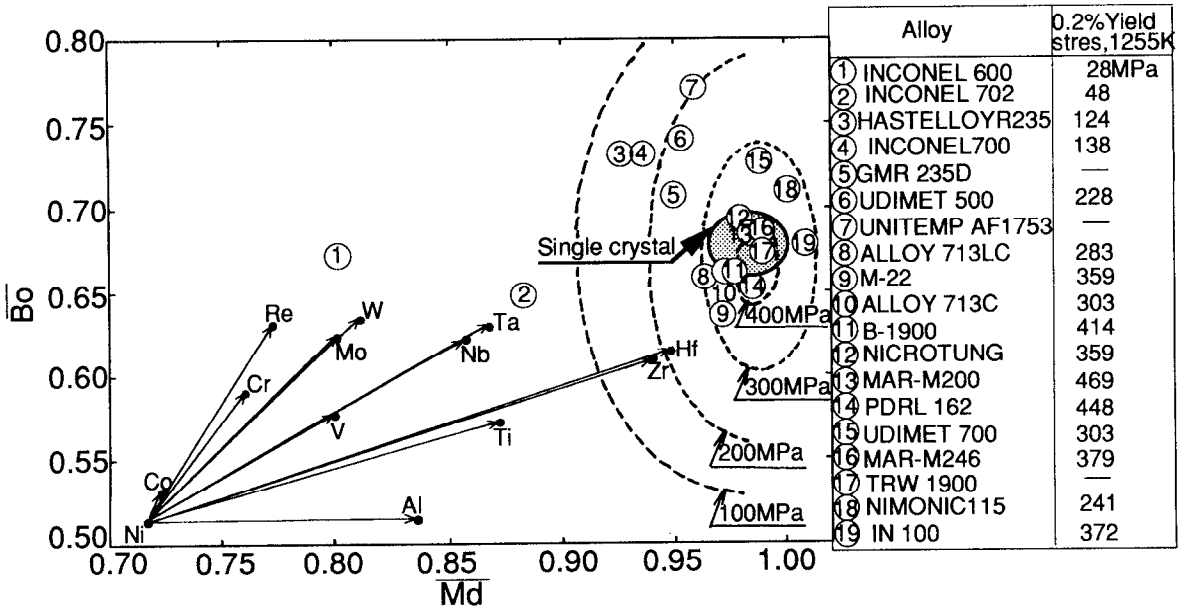

Fig.1 $\overline{Bo}$-$\overline{Md}$ diagram of showing the locations of commercial conventional cast alloys and contour lines of the 0.2% yield stress. The vectors represent the location of Ni-10 mol% M alloys.

Next, the concept of alloying vectors will be explained, because it is useful in determining the combination of alloying elements in superalloys. The vectors which represent the location of Ni-10 mol% M alloys, are shown in Fig.1, where M is alloying element. The origin of each vector is the position for pure Ni. The vector varies depending on the alloying elements. For example, it is small for Co because of the resemblance in the Md and Bo values between Ni and

Co, and large for Re because of their significant difference between Ni and Re. It is interesting to note that the directions of the vectors are similar among the elements belonging to the same group in the periodic table, for example, among Ti, Zr, Hf (4A group elements), V, Nb, Ta (5A group elements) and Cr, Mo, W (6A group elements). The alloying behavior is considered to be clearly reflected in these alloying vectors, and hence in the $\overline{Bo}$-$\overline{Md}$ diagram.

For example, as shown in Fig.2, the measured γ' solvus temperatures are plotted on the $\overline{Bo}$-$\overline{Md}$ diagram for the thirty-five alloys with the compositions of Ni-11mol%Cr-14mol%Al-(1.0~4.0)mol%Ta-(1.3~3.5)mol%W-(0~7.5)mol%Co. It was found that the iso-γ' solvus temperature lines could be drawn approximately as shown in the figure. As the γ' solvus temperatures lower from 1573K to 1513K, the iso-γ' solvus lines are shifted toward the higher $\overline{Bo}$ and the lower $\overline{Md}$ range. The slope of the iso-γ' solvus line is parallel to a vector between Ni-W and Ni-Ta, as was indicated by a dotted line in the circle. This means that the addition of V, Nb, Ta, Ti, Zr, Hf and Al into superalloys increases the γ' solvus temperature. On the contrary, the addition of Co, Re, Cr, Mo and W decreases the temperature. As shown in Fig.3, this was confimed experimentally, since the γ' solvus temperature increased with increasing Ta/W mol% ratio (9). The small change beyond the ratio of about 1.1 is simply due to the fact that such alloys fall on the γ+γ' eutectic compositional range. It is also noted that the volume fraction of the γ' phase increased with increasing Ta/W ratio.

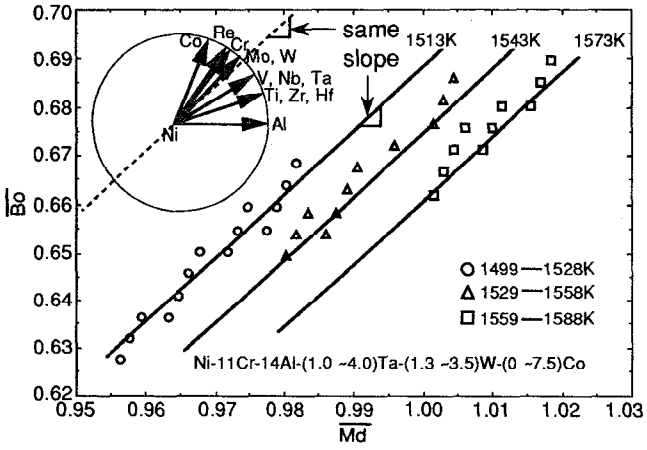

Fig.2 The representation of the γ' solvus temperatures of Ni-11Cr-14Al-(1.0~4.0)Ta-(1.3~3.5)W-(0~7.5)Co alloys in the $\overline{Bo}$-$\overline{Md}$ diagram.

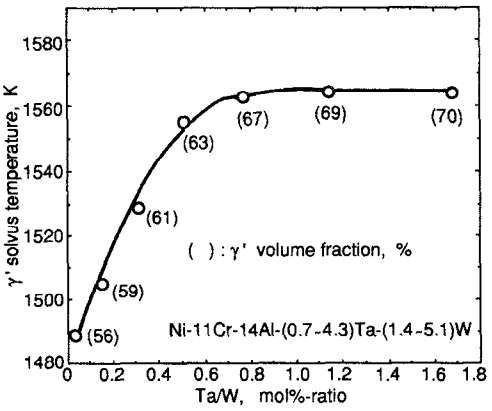

Fig.3 Correlation of Ta/W ratio with the γ' solvus temperature and γ' volume fraction in the Ni-11Cr-14Al-(0.7~4.3)Ta-(1.4~5.1)W alloys.

As explained earlier, any single crystal alloys were located in a very small $\overline{Bo}$-$\overline{Md}$ region where the 0.2% yield stress showed the maximum. In such a region the alloys probably exhibit the high γ' solvus temperature and hence the high volume fraction of the γ' phase, while keeping the good phase stability.

Alloying Effects on the High-temperature Properties

The alloying effects of Cr, Ti, Co, Re and Hf on the creep-rupture property and the hot-corrosion resistance were investigated experimentally by preparing a variety of alloys shown in Table 3. The alloy compositions were controlled so that the Md value was equal to 0.985 from the view of phase stability of alloys (5). Fig.4 shows the experimental results of the creep-rupture test at 1313K under a constant load of 137.2 MPa and of the hot-corrosion test at 1173K using a Na_2SO_4-45mol%NaCl salt.

Table 3 Compositional range of the alloys used for the present experiments on Cr,Ti,Co,Re and Hf effects.

series	compositional range, mol%									
	Ni	Cr	Al	Ti	Ta	W	Mo	Re	Co	Hf
1	bal.	10~16	12	1.2	1.2~2.7	1.2~2.9	0.4~1.0	—	—	—
2	bal.	10	12	0~2.5	1.0~3.4	3.0~3.8	—	—	—	—
3	bal.	10	12	1.5	1.9~2.1	2.1~2.3	0.7~0.8	0.25	0~9.0	—
4	bal.	10	12	1.2	2.1~2.7	1.9~2.4	0.7~0.8	0~1.0	—	—
5	bal.	10	12	1.5	2.1	2.3	0.8	0.25	—	0~0.1

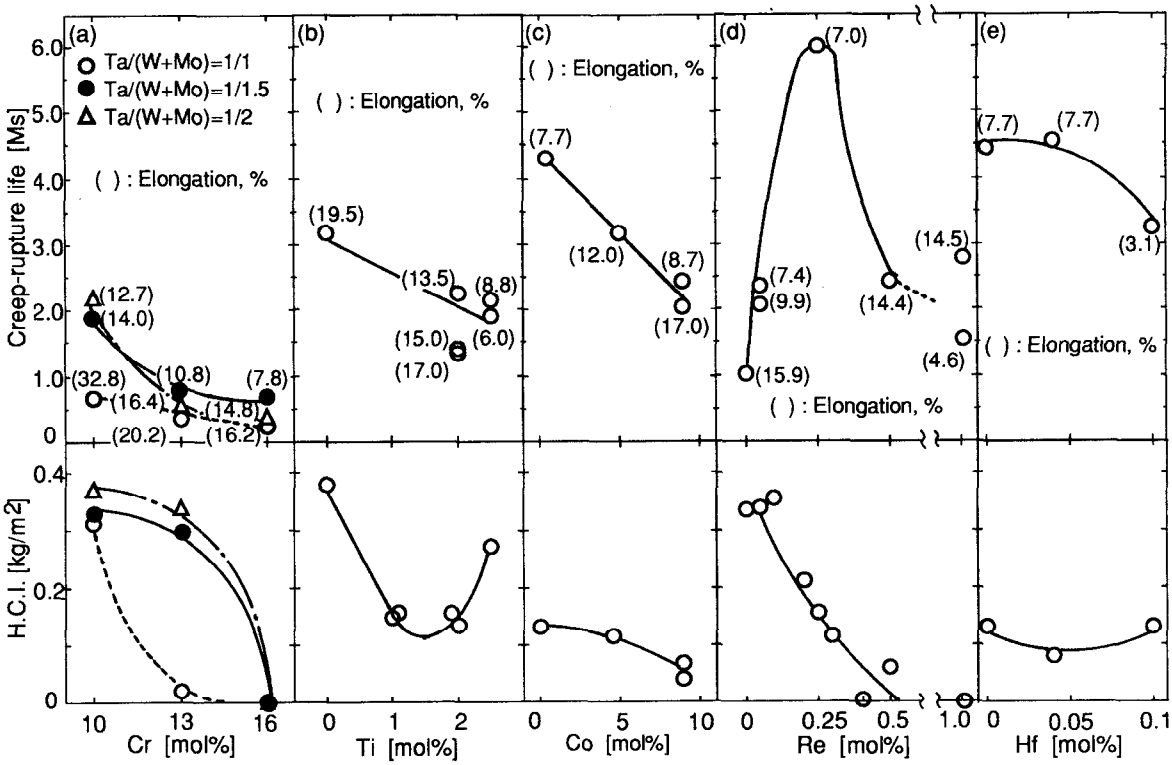

Fig.4 Effects of (a)Cr,(b)Ti,(c)Co,(d)Re,(e)Hf additions on the creep-rupture property and hot-corrosion resistance of theNi-(10~16)Cr12Al-(0~2.5)Ti-(1.0~3.4)Ta-(1.2~3.8)W-(0~1.0)Mo-(0~1.0)Re-(0~9.0)Co-(0~0.1)Hf alloys.

Effect of Cr and Co

As shown in Fig.4 (a) and (c), the creep-rupture life decreased with increasing Cr and Co contents. This decrease was probably attributable to the lowering of the γ' solvus temperatures with increasing Co and Cr contents (see Fig.2), resulting in the decrease in the γ' volume fraction in the alloys. This understanding was confirmed experimentally as shown in Fig.5. The γ' solvus temperatures measured by the differential thermal analysis decreased as the Cr and Co contents increased. Also, the measured volume fraction of the γ' phase

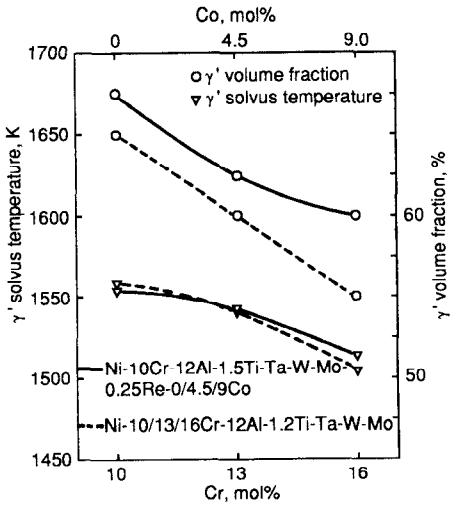

Fig.5 Changes in the γ' solvus temperature and the γ' volume fraction with Cr and Co contents.

decreased monotonously with Cr and Co contents, in agreement with the previous report (10).

The creep-ruptutre elongation was indicated by a number [%] in each parenthesis in the upper figure of Fig.4. It had a tendency of decreasing with the Cr content, but increasing with the Co content in the alloys.

The results of the hot-corrosion test are also shown in the lower figure of Fig.4. Here, the hot corrosion index (H.C.I.) is defined as the weight gain of the specimen coated with the salt and exposed to a dry-air stream for 72ks. The high H.C.I. value means the poor hot-corrosion resistance of alloys. The H.C.I. value decreased monotonously with Cr and Co contents. This result is consistent with the previous result (11,12) that the hot-corrosion resistance was improved by forming a Cr_2O_3 oxide layer on the surface.

Effect of Re

Recently great attention has been directed toward the Re containing superalloys. As shown in Fig.4 (d), for the alloys listed in Table 3, the creep-rupture life showed the maximum value at about 0.25 mol% Re. According to the chemical analysis of the γ and the γ' phases shown in Fig.6, Re was partitioned mainly into the γ phase and strengthened the γ phase. Then, the rupture life increased with Re contents up to 0.25 mol%. The decrease of the rupture life for the further increase of the Re content was interpreted as due to the poorer phase stability than the expectation from the $\overline{Md}$ values of the alloys. In order to explain this result the partitioning ratios of the elements in the γ and the γ' phases were examined from Fig.6. Cr, W, Mo and Re were distributed mainly in the γ phase, but Al, Ta and Ti were distributed mainly in the γ' phase. The Re addition reduced the content of Cr, W and Mo in the γ phase. As the Re content increases, these unsoluble elements tend to precipitate in the γ matrix, resulting in the appearance of the α phase and the σ phase in the alloys, as shown in Fig.7. Thus, the precipitation of these brittle phases deteriorated the creep-rupture life in the alloys containing more than 0.4 mol% Re, as shown in Fig.4 (d). In addition, it is apparent from Fig.6 (b) that as the Re content increased, the Al content increased in the γ' phase, but the Ta content decreased reversely in the γ' phase.

These experimental results imply that in order to keep the phase stability good, compositional adjustment is needed among the elements having the alloying vectors of similar directions, so that their total amount is kept under a certain level. Such an example may be seen in the PWA 1480 (the first generation alloy) and the PWA 1484 (the second generation alloy). Compared to PWA 1480, the Cr content of PWA 1484 was reduced to 6 mol%, wheras the Re content was increased by 1 mol% Re. Thus, the Cr and Re contents are changed in a reverse way, as their alloying vectors are toward the similar direction. Also the Al content of PWA 1484 increased, but the contents of both Ti and Ta decreased. Such a balancing of elements is consistent with the concept of alloying vectors and also with the experimental result shown in Fig.6. In addition, the partitioning of elements between the γ and γ' phases correlates with the alloying vectors. For example, all the elements of partitioning mainly into the γ phase (Cr, W, Mo and Re) have the vector direction higher than the slope of the iso-γ' solvus line (i.e., the dotted line in the circle in Fig.2).

On the other hand, no clear correlation was observed between the creep-rupture elongation and Re content. Also, it was found that the H.C.I. value was reduced to nearly nil by the addition of 0.4~0.5 mol% Re.

Most of alloying elements in superalloys can enhance either the creep-rupture strtength or the hot-corrosion resistance, but never enhance the both properties. However, Re is an exceptional element since it could enhance the both properties as far as the good phase stability is

kept by the alloying.

Effect of Ti and Hf

Ti has been added in the superalloys in order to improve the hot- corrosion resistance against a sea salt and also to strengthen the γ phase. On the other hand, Hf has been known as the element strengthening the grain boundary, but recently it has been added even in the single cryatal superalloys in order to improve the oxidation resistance (13). However, as shown in Fig.4 (b) and (e), the creep-rupture life decreased with increasing Ti and Hf contents in the alloys.

The creep-rupture elongation had a tendency of decreasing with increasing Ti and Hf contents. Also, the H.C.I. value showed the minimum value at 1.5 mol% Ti and 0.035 mol% Hf.

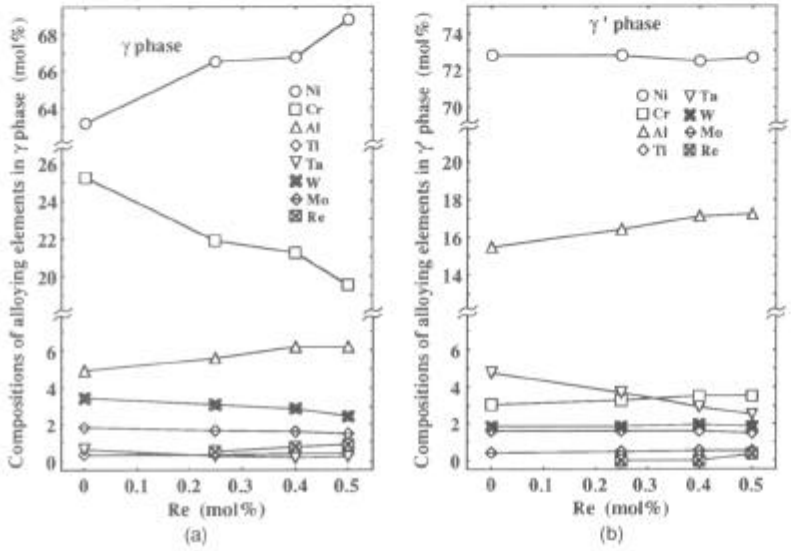

Fig.6 Changes in the chemical compositions of (a)the γ phase and (b)the γ' phase with the Re content in the Ni-10Cr-12Al-1.2Ti-(2.1~2.7)Ta-(1.9~2.4)W-(0.7~0.8)Mo-(0~0.5)Re alloys.

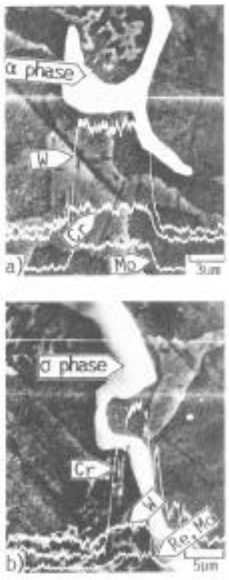

Fig.7 SEM images of showing a)the α phase and b)the σ phase precipitated in the Ni-10Cr-12Al-1.2Ti-2.6Ta-1.9W-0.7Mo-0.4Re alloy.

Discussion

Realistic Advancement of Single Crystal Superalloys

As mentioned above, $\overline{Bo}$-$\overline{Md}$ diagram is quite useful for design of nickel-based superalloys. On the basis of the $\overline{Bo}$-$\overline{Md}$ diagram, alloy chemistry was treated of the twenty-one single crystal superalloys developed so far in the world. The region of single crystals plotted in Fig.1 is enlarged in Fig.8. In this figure, only the directions of the alloying vectors are also represented in a circle. Furthermore, the creep-rupture life and the H.C.I. value are listed for the alloys. The limits for the suppression of both the α-W(Mo) phase and the eutectic γ' phase formation were determined from experiments (6). The area between the limits was regarded as the region where single crystal superalloys could keep the good phase stability. From this meaning, in TMS alloys (TMS 12-1, -12, -26) and SC alloys (SC-53A, -83) locating outside the region, the α-W(Mo) phase must precipitate, resulting in the poor hot-corrosion resistance. On the other hand, for the alloys (for example PWA 1480) locating outside the limit for the eutectic γ' phase (see Fig.8), the

creep-rupture lives were rather short. Thus, alloy design should be performed within the limits shown in Fig.8. In particular, the area having the high $\overline{Md}$ and the high $\overline{Bo}$ values within the limits may be favorable for getting high performance alloys. In fact, TUT 31D and TUT 95 alloys of containing 0.25 mol% Re are located in such a region. However, PWA 1484 and CMSX-4/4G alloys of containing 1 mol% Re are located in the lower $\overline{Bo}$ and $\overline{Md}$ region.

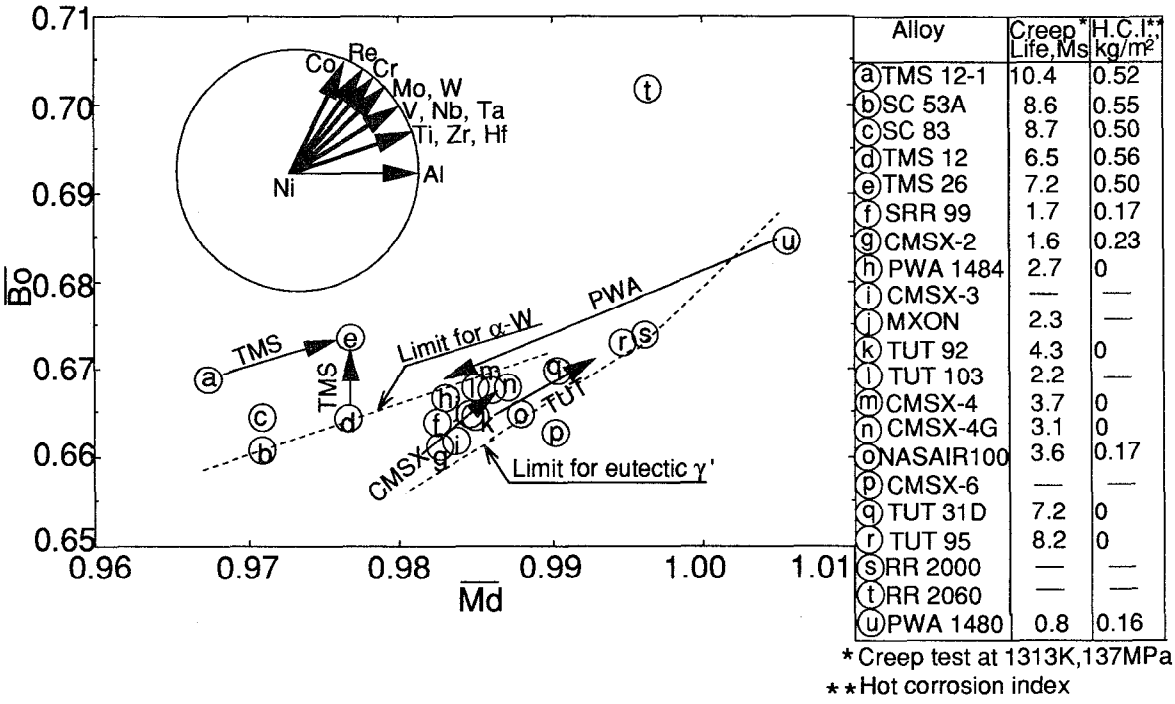

Alloy	Creep* Life,Ms	H.C.I** kg/m²
ⓐTMS 12-1	10.4	0.52
ⓑSC 53A	8.6	0.55
ⓒSC 83	8.7	0.50
ⓓTMS 12	6.5	0.56
ⓔTMS 26	7.2	0.50
ⓕSRR 99	1.7	0.17
ⓖCMSX-2	1.6	0.23
ⓗPWA 1484	2.7	0
ⓘCMSX-3	—	—
ⓙMXON	2.3	—
ⓚTUT 92	4.3	0
ⓛTUT 103	2.2	—
ⓜCMSX-4	3.7	0
ⓝCMSX-4G	3.1	0
ⓞNASAIR100	3.6	0.17
ⓟCMSX-6	—	—
ⓠTUT 31D	7.2	0
ⓡTUT 95	8.2	0
ⓢRR 2000	—	—
ⓣRR 2060	—	—
ⓤPWA 1480	0.8	0.16

* Creep test at 1313K,137MPa
** Hot corrosion index

Fig.8 Locations of various single crystal superalloys in the $\overline{Bo}$-$\overline{Md}$ diagram.

Alloy Modification

The alloys may be modified using the alloying vectors in the d-electrons concept. For example, the advancement from PWA 1480 to PWA 1484 will be examined first. From Table 1 the compositional differences between two alloys will be summarized as follows;
1)+2.0 mol% Al, 2)+1.0 mol% Re, 3)+1.3 mol% Mo, 4)+0.7 mol% W, 5)-1.0 mol% Ta, 6)-1.9 mol% Ti, 7)-6.0 mol% Cr, 8)+5.8 mol% Co, 9)+0.04 mol% Hf.
Here, + sign indicates that the composition is higher in PWA 1484 than in PWA 1480, and - sign indicates the reverse meaning. In Fig.9, the corresponding sequence of alloy modification is shown by the vectors, starting from①for PWA 1480.

For instance, the addition of only +2.0 mol% Al into PWA1480 shifts the alloy position from①to② . The further addition of +1.0 mol% Re changes the position from②to③ . Such a step is repeated until the end of ⑩ for PWA 1484. It is evident that the large change from⑦to⑧ due to the decrease of the Cr content is compensated for the changes from 2 to 5 due to the increase of the Re, Mo and W contents. Also, the change due to the increase of the Al content is compensated in part for the change due to the decrease of the Ti and Ta contents in the alloy. The small change in the position from⑧to⑨is seen in this diagram even by the large change in the Co content, because of the small alloying vector for Co.

This alloy modification from PWA 1480 to PWA 1484 has improved both the creep-rupture property and the hot-corrosion resistance. Also, there was not the residual eutectic γ' phase in PWA 1484 after solution-heat treatment, whereas it was retained by about 4 volume percent in PWA 1480. However, the creep-rupture life of PWA 1484 is still shorter, compared to that of

CMSX-4 despite of both alloys containing the same amount of Re, 1 mol%. The further modification of PWA 1484 may be necessary in order to increase the creep-rupture life as long as the CMSX-4. So, by setting the target values of the $\overline{Bo}$ and $\overline{Md}$ close to those of CMSX-4, a simulation was carried out for the minor modification of PWA 1484.

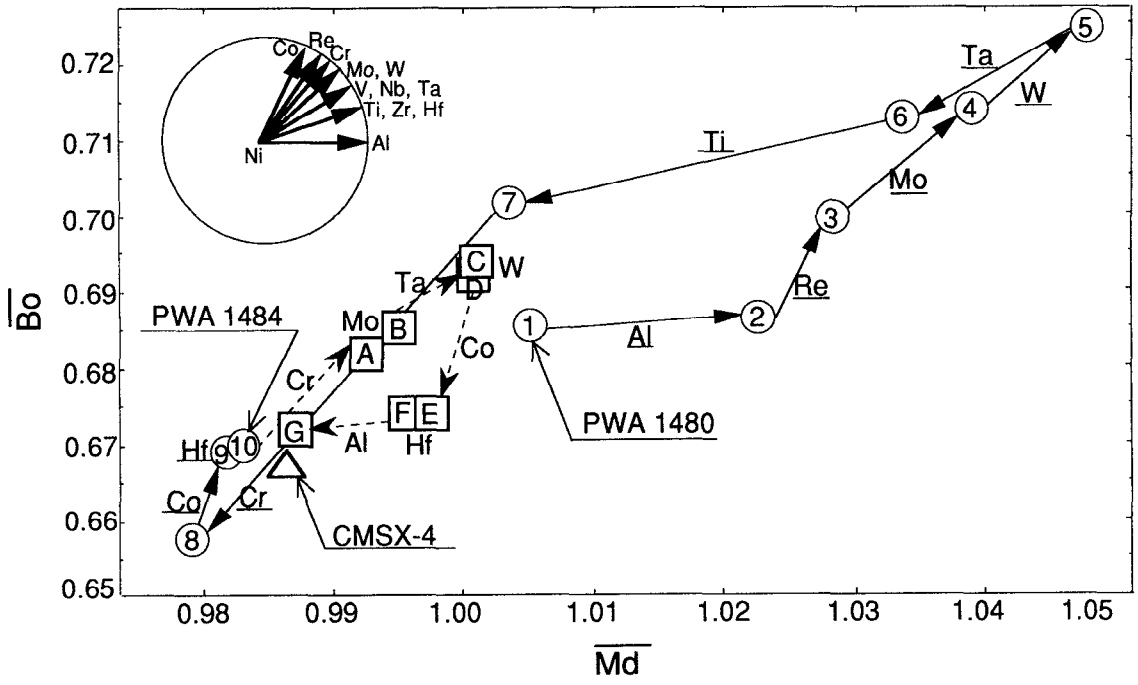

Fig.9 Modification of the PWA alloys using the $\overline{Bo}$-$\overline{Md}$ diagram.

Firstly, the Re content was fixed at 1 mol%, and Co was set free, since the creep-rupture life decreased by the addition of Co into superalloys as shown in Fig.4 (c). Each step of the modification is indicated by the vector on the broken line in Fig.9. It starts from ⑩ for PWA 1484 and ends at G for a promising modified alloy. Each step between them is summarized as follows;

⑩→ A: increase of Cr content for the improvement of the hot-corrosion resistance,

A→ B: increase of Mo content for the strengthening of the γ phase and for the lowering of the alloy density by substituting Mo for W,

B→ C: increase of Ta content for the strengthening of the γ' phase and for the increase of the γ' volume fraction and the γ' solvus temperature,

C→ D: decrease of W content for the suppression of the formation of the α-W phase formation and also for the decrease of the alloy density,

D→ E: decrease of Co content for the increase of the solubility of the refractory metals such as W, Mo and Re,

E→ F: removal of Hf for the increase of the solubility of the refractory metals while keeping the good phase stability,

F→ G: decrease of Al content for the substitution of Ta for Al and for the strengthening of the γ' phase by Ta.

Conclusion

It was proved that the d-electrons concept was useful in understanding alloying effects

on the high-temperature properties and also in considering the realistic advancement and the future for single crystal superalloys.

Acknowledgments

We would like to express sincere thanks to Messrs. R.Yokoyama, Y.Kawamura, H.Ishihara, S.Miyazaki and Y.Harada for their experimental assistance. This research was supported in part by Grant-in Aid for Scientific Research from the Ministry of Education, Science and Culture of Japan.

References

1. M.Morinaga, N,Yukawa and H.Adachi, "Alloying Effect on The Electronic Structure of $Ni_3Al(\gamma')$", J. Phys. Soc. Jpn., 53(2)(1984), 653-663.
2. M.Morinaga, N.Yukawa,H.Adachi and H.Ezaki,"New PHACOMP and its Application to Alloy Design", Proc.5th Int. Symp. on Superalloys, ed. M.Gell et al. (Warrendale, PA : The Metallugical Society of AIME, 1984), 523-532.
3. M.Morinaga, N.Yukawa, H.Ezaki and H.Adachi, "Solid Solubilities in Transition-Metal-based f.c.c. Alloys", Phil. Mag. A, 51(2)(1985),223-246.
4. M.Morinaga, N.Yukawa, H.Ezaki and H.Adachi, "Solid Solubilities in Nickel-based f.c.c.Alloys", Phil. Mag. A, 51(2)(1985), 247-252.
5. N.Yukawa, M.Morinaga, Y.Murata, H.Ezaki and S.Inoue,"High Performance Single Crystal Superalloys Developed by the d-electerons Concept", Proc. 6th Int.Symp.on Superalloys, ed. D.N.Duhl et al.(Warrendale, PA : the Metallurgical Society, Inc., 1988), 225-234.
6. K.Matsugi, R.Yokoyama, Y.Murata, M.Morinaga and N.Yukawa, "High-temperature Properties of Single Crystal Superalloys Optimized by an Electron Theory", Proc. 4th Int. Conf. on High Temperature Materials for Power Engineering 1990, ed. E.Bachelet et al. (Dordrecht, Netherlands : Kluwer Academic Publishers, 1990), 1251-1261.
7. J.C.Slater, The Calculation of Molecular Orbitals, John-Wily & Sons, Inc., New York, 1979.
8. Catalog of High Temperature High Strength Nickel Base Alloys, the International Nickel Company, Inc., 67 Wall Street, New York, N.Y.10005, 1964.
9. K.Matsugi, Y.Murata, M.Morinaga and N.Yukawa, "Correlation of Ta/W Compositional Ratios with the High Temperature Properties of Ni-Cr-Al-Ta-W(-Co) Single Crystal Superalloys", J. Iron and Steel Inst. Jpn., 78 (4) (1992), 666-672.
10. M.V.Nathal and L.J.Ebert,"The Influence of Cobalt, Tantalum, and Tungsten on the Microstructure of Single Crystal Nickel-Base Superalloys", Metall. Trans. A, 16(10)(1985), 1849-1862.
11. J.A.Goebel and F.S.Pettit,"Na2SO4-Induced Accelerated Oxidation (Hot-Corrosion) of Nickel", Metall. Trans., 1(7)(1970), 1943-1954.
12. M.Kawakami, K.S.Goto, R.A.Rapp and F.Kajiyama,"Mechanism of Accelerated Oxidation of Heat Resistant Super Alloys Induced by Molten Salt Deposition", J. Iron and Steel Inst. Jpn., 65 (7) (1979), 811-819.
13. D.J.Frasier, J.R.Whetstone, K.Harris, G.L.Erickson and R.E.Schwer,"Process and Alloy Optimization for CMSX-4 Superalloy Single Crystal Airfoils",Proc.4th Int. Conf. on High Temperature Materials for Power Engineering 1990, (1990), 1281-1300.